Universität Karlsruhe (TH)
Institut für Baustatik

# A Geometrical Nonlinear Eccentric 3D–Beam Element with Arbitrary Cross–Sections

F. Gruttmann, R. Sauer, W. Wagner

Mitteilung 2(1996)

Universität Karlsruhe (TH)
Institut für Baustatik

# A Geometrical Nonlinear Eccentric 3D–Beam Element with Arbitrary Cross–Sections

**F. Gruttmann, R. Sauer, W. Wagner**

**Mitteilung 2(1996)**


Prof. Dr.–Ing. W. Wagner
Institut für Baustatik
© Universität Karlsruhe
Postfach 6980
76128 Karlsruhe

Telefon: (0721) 608–2280
Telefax: (0721) 608–6015
E–mail: bs@.uni-karlsruhe.de
Internet: http://www.bs.uni-karlsruhe.de

# A Geometrical Nonlinear Eccentric 3D–Beam Element with Arbitrary Cross–Sections

F. Gruttmann, R. Sauer and W. Wagner

*Institut für Baustatik, Universität Karlsruhe (TH), Kaiserstraße 12, D–76131 Karlsruhe, Germany*

In this paper a finite element formulation of eccentric space curved beams with arbitrary cross–sections is derived. Based on a Timoshenko beam kinematic the strain measures are derived by exploitation of the Green–Lagrangean strain tensor. Thus the formulation is conform with existing nonlinear shell theories. Finite rotations are described by orthogonal transformations of the basis systems from the initial to the current configuration. Since for arbitrary cross–sections the centroid and shear center do not coincide torsion bending coupling occurs in the linear as well as in the finite deformation case. The linearization of the boundary value formulation leads to a symmetric bilinear form for conservative loads. The resulting finite element model is characterized by 6 degrees of freedom at the nodes and therefore is fully compatible with existing shell elements. Since the reference curve lies arbitrarily to the line of centroids the element can be used to model eccentric stiffener of shells with arbitrary cross–sections.

## 1 Introduction

Three–dimensional beam–like structures undergoing large displacements and rotations occur in different areas of engineering practice. Here motions of flexible beams like helicopter blades, rotor blades, robot arms or beams in space–structure technology are mentioned. Numerous papers have been published up to now using different approaches and some of them are discussed in the following.

Due to the non–commutativity of successive finite rotations about fixed axes, Argyris et. al. introduced the so–called semi–tangential rotations to circumvent this difficulty, see [1,2,3]. The authors pointed out, that with this approach the geometric stiffness matrix becomes symmetric which is important

for the finite element formulation. An updated Lagrangean and a total Lagrangean formulation of a beam are presented for large displacements by Bathe and Bolourchi [4].

The co–rotational formulation is motivated by the fact that thin structures undergoing finite deformations are characterized by significant rigid body motions. (e.g. see Belytschko and Hsieh [5], Crisfield [6] or Nour–Omid [7]). The basis is an element–independent algorithm, where the rigid body motions (translations and rotations) are separated from the total deformation. Thus within the procedure existing linear elements are used for nonlinear computations, however usually restricted to small strains.

Several finite element formulations for three–dimensional beams are based on strain–measures derived from the principle of virtual work, Reissner [8]. The consistent linearization considering a multiplicative update procedure leads to a non–symmetric geometric tangent stiffness, which becomes symmetric at an equilibrium configuration under a conservative loading, see Simo and Vu–Quoc [9,10], Cordona and Géradin [11]. Ibrahimbegović [12] shows that the linearization ends up with symmetric matrices for an additive update of the axial vector. However this leads to a number of very complicated terms.

Most of the finite element formulations deal with beams where centroid and center of shear coincide. The problem of coupled bending torsion deformation of beams has been studied theoretically e.g. by Reissner [13,14]. In Ref. [10] torsion–warping deformation has been incorporated within the theory. The warping function is multiplied with an additional independent degree of freedom. However the resulting finite beam element with seven nodal degrees of freedom does not allow any eccentricities. An eccentric beam element with rectangular cross–sections has been developed e.g. by Weimar [15].

In this paper we aim to provide three–dimensional finite beam–elements based on a Timoshenko kinematic with transverse shear strains. The reference axis is a space curve which is independent of the line of centroids or shear center. A main goal of the paper is to retain the number of independent kinematic quantities to six. These type of elements are useful to discretize eccentric stiffener of shells.

The essential features and novel aspects of the present formulation are summarized:

(i) Based on a kinematic assumption the beam strains for finite deformations are derived by exploitation of the Green–Lagrangean strain tensor. This procedure is consistent with existing shell theories. In contrast to that, the authors of e.g. Refs. [9,10,11,12] propose finite element formulations with different beam strains.

(ii) To keep the number of independent kinematic quantities to six the warping degree of freedom is eliminated using additional constraints. The equations of Saint–Venant torsion theory along with Green's formula are applied to integrate the so–called warping coordinates. This leads to a material matrix in terms of section quantities which describes the coupling effects. Furthermore the weak form of the boundary value problem is linearized analytically which results into a symmetric bilinear form.

(iii) Much effort has been undertaken to make the beam formulation fully consistent with existing shell formulations. Thus the associated finite element formulation is characterized by the fact, that the six nodal degrees of freedom are identical to those of existing shell elements, see e.g. [16]. The element allows coupling of eccentric beams with thin–walled structures discretized by shell elements. Therefore the developed element can be used to discretize stiffener of shells with arbitrary cross–sections.

The contents of the paper is outlined as follows:
Based on a kinematic assumption the beam strains are derived from the Green–Lagrangean strain tensor in the next section. The underlying variational formulation in a Lagrangean representation is depicted in section 3. The associated weak formulation of the boundary value problem is written in terms of stress–resultants. It is shown, that the variational equations can be rewritten with transformed stress–resultants. This leads to work conjugate beam strains which have been discussed in the literature. Furthermore the linearized boundary value problem is given. Assuming linear elastic behaviour the constitutive equations in terms of stress resultants are derived in section 4. In section 5 the associated finite element formulation using Lagrangean interpolation functions is presented. Several numerical examples are presented in section 6. Comparisons of our results are made if possible with those reported in the literature. Further comparisons are given, where the beams are discretized with shell elements.

## 2 Kinematic description of the beam

In this section we consider a beam with reference configuration denoted by $\mathcal{B}_0$, see Fig. 1. We introduce the orthogonal basis system $\mathbf{A}_i = \mathbf{R}_0\,\mathbf{e}_i$ with associated coordinates $\{\xi_1, \xi_2, \xi_3\}$ where $\mathbf{e}_i$ denotes the fixed cartesian basis system. The axis of the beam is initially along $\mathbf{A}_1$ with the arc–length parameter $S = \xi_1 \in [0, L]$ of the spatial curve. The cross–sections of the beam therefore lie in planes described by the basis vectors $\{\mathbf{A}_2, \mathbf{A}_3\}$.

The position vectors of the undeformed and deformed cross–sections are given

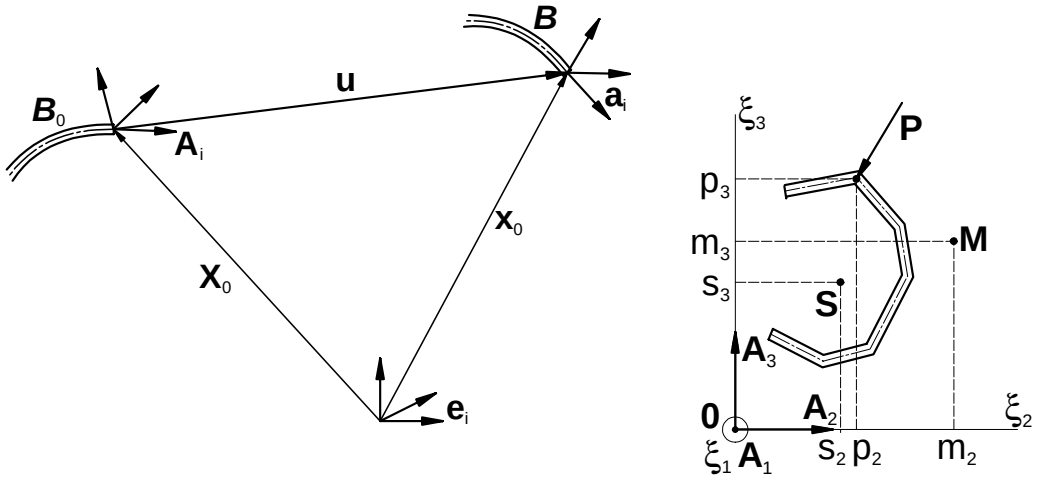


Fig. 1. Initial and current configuration of the beam, definition of the reference basis, $\mathbf{e}_i$ and $\mathbf{A}_i$ and the current frame $\mathbf{a}_i$

with the following kinematic assumption

$$\begin{aligned}\mathbf{X}(\xi_2,\xi_3,S) &= \mathbf{X}_0(S) + \xi_2\mathbf{A}_2(S) + \xi_3\mathbf{A}_3(S)\\ \mathbf{x}(\xi_2,\xi_3,S,t) &= \mathbf{x}_0(S,t) + \xi_2\mathbf{a}_2(S,t) + \xi_3\mathbf{a}_3(S,t) + \alpha(S,t)\,\tilde{w}(\xi_2,\xi_3)\,\mathbf{a}^1(S,t)\end{aligned} \tag{1}$$

with $\mathbf{a}^1\cdot\mathbf{x}_0' = 1$ and $\mathbf{a}^1\cdot\mathbf{a}_\beta = 0$ where $\beta = 2,3$. First $\alpha(S,t)$ is an independent kinematic quantity which will be eliminated using additional constraints.

The basis vectors $\mathbf{A}_i$ and $\mathbf{a}_i$ are orthonormal and are obtained from

$$\mathbf{A}_i = \mathbf{R}_0\,\mathbf{e}_i\,, \qquad \mathbf{a}_i = \mathbf{R}\,\mathbf{e}_i\,, \tag{2}$$

where the tensors $\mathbf{R}_0, \mathbf{R} \in SO(3)$ fulfill $\mathbf{R}_0^T\mathbf{R}_0 = \mathbf{1}$ and $\mathbf{R}^T\mathbf{R} = \mathbf{1}$, respectively. Thus the derivatives of $\mathbf{A}_i$ and $\mathbf{a}_i$ can be expressed as

$$\mathbf{A}_i' = \boldsymbol{\theta}_0 \times \mathbf{A}_i \qquad \mathbf{a}_i' = \boldsymbol{\theta} \times \mathbf{a}_i \tag{3}$$

where we use the customary symbol $(\cdot)'$ to denote the differentiation $\partial/\partial\xi_1 = \partial/\partial S$. Several representations of orthogonal tensors using Eulerian angles, Cardan angles, quaternions etc. have been discussed in the literature, see e.g. Argyris [17], Géradin et.al. [18]. The rotation tensor and the derivative with respect to $S$ are specified in appendix A.1.

The warping function $\tilde{w}(\xi_2,\xi_3)$ is defined within the Saint–Venant torsion theory for beams. The equilibrium equations and boundary conditions of a prismatical beam with cross–section $A$ and with the outward normal vector $\mathbf{n} = [n_2, n_3]^T$ along the boundary $C$ subjected to torsion yields the following

equations, see e.g. Sokolnikoff [19]

$$\begin{aligned} &\tilde{w}_{,22} + \tilde{w}_{,33} = 0 && \text{in} \quad A \\ &\tilde{w}_{,2}\, n_2 + \tilde{w}_{,3}\, n_3 = (\xi_3 - m_3) n_2 - (\xi_2 - m_2) n_3 && \text{on} \quad C\,. \end{aligned} \tag{4}$$

Here the notation $(\cdot)_{,i}$ is used to denote partial derivatives with respect to the coordinates $\xi_i$. The solution of the Neumann problem (4) along with the normality conditions

$$\int\limits_{(A)} \tilde{w}\, dA = 0\,, \qquad \int\limits_{(A)} \tilde{w}\, \xi_2\, dA = 0\,, \qquad \int\limits_{(A)} \tilde{w}\, \xi_3\, dA = 0 \tag{5}$$

defines the shear center $M$ with coordinates $\{m_2, m_3\}$.

Hence the derivatives of the position vectors with respect to the coordinates $\xi_1, \xi_2, \xi_3$ lead to

$$\begin{aligned} \mathbf{X}_{,1} &= \mathbf{X}_0' + \xi_2 \mathbf{A}_2' + \xi_3 \mathbf{A}_3' & \mathbf{x}_{,1} &= \mathbf{x}_0' + \xi_2 \mathbf{a}_2' + \xi_3 \mathbf{a}_3' + \tilde{w}\,(\alpha' \mathbf{a}^1 + \alpha\, \mathbf{a}'^1) \\ \mathbf{X}_{,2} &= \mathbf{A}_2 & \mathbf{x}_{,2} &= \mathbf{a}_2 + \alpha\, \tilde{w}_{,2}\, \mathbf{a}^1 \\ \mathbf{X}_{,3} &= \mathbf{A}_3 & \mathbf{x}_{,3} &= \mathbf{a}_3 + \alpha\, \tilde{w}_{,3}\, \mathbf{a}^1 \end{aligned} \tag{6}$$

The tangent vectors $\mathbf{G}_i = \mathbf{X}_{,i}$ and $\mathbf{g}_i = \mathbf{x}_{,i}$ are inserted into the Green–Lagrangean strain tensor $\mathbf{E} = E_{ij} \mathbf{G}^i \otimes \mathbf{G}^j$. The components with respect to the dual basis system $\mathbf{G}^i$ defined by $\mathbf{G}_i \cdot \mathbf{G}^j = \delta_i^j$ read

$$E_{ij} = \frac{1}{2} \left( \mathbf{x}_{,i} \cdot \mathbf{x}_{,j} - \mathbf{X}_{,i} \cdot \mathbf{X}_{,j} \right). \tag{7}$$

Using matrix notation the non–vanishing components of the Green–Lagrangean strain tensor read

$$\mathbf{E} = \bar{\mathbf{A}}\, \bar{\mathbf{E}} \tag{8}$$

where

$$\mathbf{E} = \begin{bmatrix} E_{11} \\ 2E_{12} \\ 2E_{13} \end{bmatrix}, \quad \bar{\mathbf{A}} = \begin{bmatrix} 1 & \xi_3 & \xi_2 & 0 & 0 & 0 & 0 & \tilde{w} \\ 0 & 0 & 0 & 1 & 0 & -\xi_3 & \tilde{w}_{,2} & 0 \\ 0 & 0 & 0 & 0 & 1 & \xi_2 & \tilde{w}_{,3} & 0 \end{bmatrix}, \quad \bar{\mathbf{E}} = \begin{bmatrix} \hat{\mathbf{E}} \\ \alpha \\ \alpha' \end{bmatrix} \tag{9}$$

and

$$\hat{\mathbf{E}} = \begin{bmatrix} \varepsilon \\ \kappa_2 \\ \kappa_3 \\ \gamma_2 \\ \gamma_3 \\ \vartheta \end{bmatrix} = \begin{bmatrix} \frac{1}{2}(\mathbf{x}_0' \cdot \mathbf{x}_0' - \mathbf{X}_0' \cdot \mathbf{X}_0') \\ \mathbf{x}_0' \cdot \mathbf{a}_3' - \mathbf{X}_0' \cdot \mathbf{A}_3' \\ \mathbf{x}_0' \cdot \mathbf{a}_2' - \mathbf{X}_0' \cdot \mathbf{A}_2' \\ \mathbf{x}_0' \cdot \mathbf{a}_2 - \mathbf{X}_0' \cdot \mathbf{A}_2 \\ \mathbf{x}_0' \cdot \mathbf{a}_3 - \mathbf{X}_0' \cdot \mathbf{A}_3 \\ \mathbf{a}_2' \cdot \mathbf{a}_3 - \mathbf{A}_2' \cdot \mathbf{A}_3 \end{bmatrix}. \tag{10}$$

Here we make use of the relation $\mathbf{a}_2' \cdot \mathbf{a}_3 = -\mathbf{a}_3' \cdot \mathbf{a}_2 = \boldsymbol{\theta} \cdot \mathbf{a}_1$. Note, that products of $\xi_\beta, \tilde{w}, \alpha, \alpha'$ and $\mathbf{x}_0' \cdot \mathbf{a}'^1$ of higher order are neglected in (9). This is justified for thin beams undergoing small strains. A comparison with other beam strains is given in section 3.1.

Our main goal is to keep the number of independent degrees of freedom to six. This can be achieved introducing the following constraints:

$$M_w = C_M \, \alpha' = 0 \qquad \text{and} \qquad \alpha = \vartheta \tag{11}$$

where $M_w$ and $C_M = \int_A \tilde{w}^2 \, \mathrm{d}A$ denote the so–called bi–moment and warping constant, respectively. Numerical examples show in many cases that for elasticity the contribution of the bi–moment to the stored energy is neglectable. However, it should be emphasized that this does not hold in any case.

Hence relation (8) is simplified using the constraints (11)

$$\mathbf{E} = \mathbf{A}\hat{\mathbf{E}} \qquad \text{and} \qquad \mathbf{A} = \begin{bmatrix} 1 & \xi_3 & \xi_2 & 0 & 0 & 0 \\ 0 & 0 & 0 & 1 & 0 & -\tilde{\xi}_3 \\ 0 & 0 & 0 & 0 & 1 & \tilde{\xi}_2 \end{bmatrix} \tag{12}$$

with the modified coordinates $\tilde{\xi}_2 = \xi_2 + \tilde{w}_{,3}$ and $\tilde{\xi}_3 = \xi_3 - \tilde{w}_{,2}$.

## 3 Variational formulation

In the following the virtual works of the stresses and the external forces are derived for the beam kinematics. For this purpose stress resultants and stress couple resultants are defined. The linearization of the weak form of equilibrium is derived analytically which leads to a symmetric bilinear form for conservative loading.

### 3.1 Virtual works of stress resultants and external forces

Starting with the equilibrium in weak form of a body $\mathcal{B}$ in a Lagrangean setting we obtain

$$G(\mathbf{u}, \delta\mathbf{u}) = \int_{\mathcal{B}_0} \mathbf{S} \cdot \delta\mathbf{E} \, \mathrm{d}V - \int_{\mathcal{B}_0} \rho_0 \hat{\mathbf{b}} \cdot \delta\mathbf{u} \, \mathrm{d}V - \int_{\partial\mathcal{B}_0} \hat{\mathbf{t}} \cdot \delta\mathbf{u} \, \mathrm{d}\Omega = 0 \tag{13}$$

where $\rho_0\hat{\mathbf{b}}$ and $\hat{\mathbf{t}}$ are applied body forces and surface forces, respectively. The Green–Lagrangean strain tensor is work conjugate to the Second Piola–Kirchhoff stress tensor $\mathbf{S} = S^{ij}\,\mathbf{G}_i \otimes \mathbf{G}_j$. Within the beam theory the components $S^{22}, S^{33}, S^{23}$ are assumed to be zero. The independent kinematic quantities of the beam are $\mathbf{v} = [\mathbf{u}, \mathbf{R}]^T$. Here $\mathbf{u} = \mathbf{x}_0 - \mathbf{X}_0$ and $\mathbf{R} = \mathbf{a}_i \otimes \mathbf{e}_i$ denote the displacement vector and the rotation tensor of the reference curve according to (1), respectively. Hence the space of kinematically admissible variations is introduced by

$$\mathcal{V} := \{\delta\mathbf{v} = [\delta\mathbf{u}, \delta\mathbf{w}]^T : [0, L] \longrightarrow R^3 | \quad \delta\mathbf{v} = \mathbf{0} \quad \text{on} \quad \mathcal{S}_u\} \tag{14}$$

where $\mathcal{S}_u$ describes the boundaries with prescribed displacements and rotations.

First the internal virtual work $G_{int}$ considering (12) and $S^{22} = S^{33} = S^{23} = 0$ is reformulated

$$G_{int} = \int_{\mathcal{B}_0} \mathbf{S} \cdot \delta\mathbf{E} \, \mathrm{d}V = \int_S \delta\hat{\mathbf{E}}^T \hat{\mathbf{S}} \, \mathrm{d}S \tag{15}$$

which defines the vector of stress resultants

$$\hat{\mathbf{S}} = \begin{bmatrix} N \\ M^2 \\ M^3 \\ Q^2 \\ Q^3 \\ M^1 \end{bmatrix} = \int_A \begin{bmatrix} S^{11} \\ S^{11}\xi_3 \\ S^{11}\xi_2 \\ S^{12} \\ S^{13} \\ S^{13}\tilde{\xi}_2 - S^{12}\tilde{\xi}_3 \end{bmatrix} \mathrm{d}A \tag{16}$$

and the work conjugate beam strains

$$\delta\hat{\mathbf{E}} = \begin{bmatrix} \delta\varepsilon \\ \delta\kappa_2 \\ \delta\kappa_3 \\ \delta\gamma_2 \\ \delta\gamma_3 \\ \delta\vartheta \end{bmatrix} = \begin{bmatrix} \mathbf{x}_0' \cdot \delta\mathbf{u}' \\ \mathbf{a}_3' \cdot \delta\mathbf{u}' + \mathbf{x}_0' \cdot \delta\mathbf{a}_3' \\ \mathbf{a}_2' \cdot \delta\mathbf{u}' + \mathbf{x}_0' \cdot \delta\mathbf{a}_2' \\ \mathbf{a}_2 \cdot \delta\mathbf{u}' + \mathbf{x}_0' \cdot \delta\mathbf{a}_2 \\ \mathbf{a}_3 \cdot \delta\mathbf{u}' + \mathbf{x}_0' \cdot \delta\mathbf{a}_3 \\ \mathbf{a}_1 \cdot \delta\boldsymbol{\theta} + \boldsymbol{\theta} \cdot \delta\mathbf{a}_1 \end{bmatrix} \tag{17}$$

The variation of the basis vector $\mathbf{a}_i$ and subsequent derivative with respect to the arc–length follows from (2)

$$\begin{aligned} \delta\mathbf{a}_i &= \delta\mathbf{w} \times \mathbf{a}_i \\ \delta\mathbf{a}_i' &= \delta\mathbf{w}' \times \mathbf{a}_i + \delta\mathbf{w} \times \mathbf{a}_i' \\ \delta\mathbf{w}' &= \delta\boldsymbol{\theta} - \delta\mathbf{w} \times \boldsymbol{\theta} \end{aligned} \tag{18}$$

Eq. $(18)_3$ is proofed in appendix A.2.

Thus introducing the matrix differential operator $\mathbf{L}$ one obtains the variation of the strain vector

$$\delta\hat{\mathbf{E}} = \mathbf{H}\,(\mathbf{L}\,\delta\mathbf{v}) \qquad \mathbf{H} = \begin{bmatrix} \mathbf{x}_0'^T & \mathbf{0} & \mathbf{0} \\ \mathbf{a}_3'^T & \mathbf{b}_3'^T & \mathbf{b}_3^T \\ \mathbf{a}_2'^T & \mathbf{b}_2'^T & \mathbf{b}_2^T \\ \mathbf{a}_2^T & \mathbf{b}_2^T & \mathbf{0} \\ \mathbf{a}_3^T & \mathbf{b}_3^T & \mathbf{0} \\ \mathbf{0} & \mathbf{0} & \mathbf{a}_1^T \end{bmatrix} \qquad \mathbf{L} = \begin{bmatrix} \dfrac{\mathrm{d}}{\mathrm{d}S}\mathbf{1} & \mathbf{0} \\ \mathbf{0} & \mathbf{1} \\ \mathbf{0} & \dfrac{\mathrm{d}}{\mathrm{d}S}\mathbf{1} \end{bmatrix} \tag{19}$$

with the definitions $\mathbf{b}_i := \mathbf{a}_i \times \mathbf{x}_0'$ and $\mathbf{b}_i' := \mathbf{a}_i' \times \mathbf{x}_0'$.

Next the external virtual work is specified for the beam configuration. The body forces $\rho_0\hat{\mathbf{b}}$ are neglected in the following. Furthermore we assume external loads $\hat{\mathbf{p}} = \hat{\mathbf{p}}(S)$ acting at the coordinates $\{\xi_2, \xi_3\} = \{p_2, p_3\}$, see Fig. 1. In this case the variation reads

$$G_{ext}(\mathbf{v}, \delta\mathbf{v}) = -\int_S \hat{\mathbf{p}} \cdot \delta\mathbf{x}_P \,\mathrm{d}S \tag{20}$$

with $\mathbf{x}_P = \mathbf{x}_0 + p_2\,\mathbf{a}_2 + p_3\,\mathbf{a}_3$. Thus applying $(18)_1$ yields

$$\begin{aligned} G_{ext}(\mathbf{v}, \delta\mathbf{v}) &= -\int_S \hat{\mathbf{p}} \cdot (\delta\mathbf{u} + p_2\,\delta\mathbf{a}_2 + p_3\,\delta\mathbf{a}_3)\,\mathrm{d}S \\ &= -\int_S (\hat{\mathbf{p}} \cdot \delta\mathbf{u} + \hat{\mathbf{m}} \cdot \delta\mathbf{w})\,\mathrm{d}S \end{aligned} \tag{21}$$

with $\hat{\mathbf{m}} = \mathbf{d} \times \hat{\mathbf{p}}$ and $\mathbf{d} = p_2\,\mathbf{a}_2 + p_3\,\mathbf{a}_3$.

Hence the weak form of equilibrium (13) considering (15) and (21) can be rewritten

$$\begin{aligned} G(\mathbf{v}, \delta\mathbf{v}) &= \int_S \left[\mathbf{f} \cdot \delta\mathbf{u}' + (\mathbf{f} \times \mathbf{x}_0') \cdot \delta\mathbf{w} + \mathbf{m} \cdot \delta\mathbf{w}'\right] \mathrm{d}S - \int_S (\hat{\mathbf{p}} \cdot \delta\mathbf{u} + \hat{\mathbf{m}} \cdot \delta\mathbf{w})\,\mathrm{d}S \\ &= \int_S (\mathbf{L}\,\delta\mathbf{v})^T \hat{\boldsymbol{\sigma}}\,\mathrm{d}S - \int_S \delta\mathbf{v}^T \hat{\mathbf{q}}\,\mathrm{d}S = 0 \end{aligned} \tag{22}$$

where

$$\hat{\boldsymbol{\sigma}} = \mathbf{H}^T \hat{\mathbf{S}} = \begin{bmatrix} \mathbf{f} \\ \mathbf{f} \times \mathbf{x}_0' \\ \mathbf{m} \end{bmatrix} \qquad \hat{\mathbf{q}} = \begin{bmatrix} \hat{\mathbf{p}} \\ \hat{\mathbf{m}} \end{bmatrix} \tag{23}$$

and the vector of stress resultants $\mathbf{f}$ and stress couple resultants $\mathbf{m}$

$$\begin{aligned} \mathbf{f} &= N\,\mathbf{x}_0' + \mathbf{n} & \mathbf{n} &= \mathbf{q} - \mathbf{l} \times \boldsymbol{\theta} & & \\ \mathbf{m} &= M^1\mathbf{a}_1 + \mathbf{l} \times \mathbf{x}_0' & \mathbf{q} &= Q^2\mathbf{a}_2 + Q^3\mathbf{a}_3 & \mathbf{l} &= M^2\mathbf{a}_3 + M^3\mathbf{a}_2\,. \end{aligned} \tag{24}$$

The local Euler–Lagrange equations are obtained integrating equation (22) by parts

$$G(\mathbf{v}, \delta\mathbf{v}) = -\int_S \left[(\mathbf{f}' + \hat{\mathbf{p}}) \cdot \delta\mathbf{u} + (\mathbf{m}' + \mathbf{x}_0' \times \mathbf{f} + \hat{\mathbf{m}}) \cdot \delta\mathbf{w}\right] \mathrm{d}S = 0 \tag{25}$$

where for simplicity we assume that the stress resultants are zero at the boundaries. Applying standard arguments the terms in brackets have to vanish, which describe the well–known equilibrium equations of a three–dimensional beam for the static case, e.g. see [20,8].

**Remark 1** *The internal virtual work can be reformulated using* (18)$_3$

$$\begin{aligned} G_{int} &= \int_S \left[\mathbf{f}\cdot(\delta\mathbf{u}' - \delta\mathbf{w}\times\mathbf{x}_0') + \mathbf{m}\cdot(\delta\boldsymbol{\theta} - \delta\mathbf{w}\times\boldsymbol{\theta})\right]\, dS \\ &= \int_S (\mathbf{F}\cdot\delta\boldsymbol{\varepsilon} + \mathbf{M}\cdot\delta\boldsymbol{\kappa})\, dS \end{aligned} \tag{26}$$

*with* $\mathbf{F} = \mathbf{R}^T\mathbf{f}$, $\mathbf{M} = \mathbf{R}^T\mathbf{m}$ *and the work conjugate strain vectors*

$$\boldsymbol{\varepsilon} = \mathbf{R}^T\mathbf{x}_0' - \mathbf{R}_0^T\mathbf{X}_0' \qquad\qquad \boldsymbol{\kappa} = \mathbf{R}^T\,\boldsymbol{\theta} - \mathbf{R}_0^T\,\boldsymbol{\theta}_0\,. \tag{27}$$

*These strain measures have been proposed by Reissner [8]. Later different parametrizations for finite element formulations have been developed by several authors, e.g. see [9,11,12]. Thus (26) shows that the internal virtual work can be written either in terms of Second Piola–Kirchhoff stress–resultants (16) or with stress–resultants* $\hat{F}^i = \mathbf{f}\cdot\mathbf{a}_i$ *and* $\hat{M}^i = \mathbf{m}\cdot\mathbf{a}_i$*. The component representation of (22) can be transformed into one of each other. The only difference which occurs follows from the used material law. The transformation between both type of stress resultants is given by*

$$\begin{bmatrix} \hat{F}^1 \\ \hat{F}^2 \\ \hat{F}^3 \\ \hat{M}^1 \\ \hat{M}^2 \\ \hat{M}^3 \end{bmatrix} = \begin{bmatrix} \mathbf{x}_0'\cdot\mathbf{a}_1 & 0\,0\,0 & \boldsymbol{\theta}\cdot\mathbf{a}_2 & \boldsymbol{\theta}\cdot\mathbf{a}_3 \\ \mathbf{x}_0'\cdot\mathbf{a}_2 & 1\,0\,0 & -\boldsymbol{\theta}\cdot\mathbf{a}_1 & 0 \\ \mathbf{x}_0'\cdot\mathbf{a}_3 & 0\,1\,0 & 0 & -\boldsymbol{\theta}\cdot\mathbf{a}_1 \\ 0 & 0\,0\,1 & -\mathbf{x}_0'\cdot\mathbf{a}_2 & -\mathbf{x}_0'\cdot\mathbf{a}_3 \\ 0 & 0\,0\,0 & \mathbf{x}_0'\cdot\mathbf{a}_1 & 0 \\ 0 & 0\,0\,0 & 0 & \mathbf{x}_0'\cdot\mathbf{a}_1 \end{bmatrix} \begin{bmatrix} N \\ Q^2 \\ Q^3 \\ M^1 \\ M^2 \\ -M^3 \end{bmatrix} \tag{28}$$

*For small strains the strain vectors approximate* $\mathbf{x}_0' \approx \mathbf{a}_1$ *and* $\boldsymbol{\theta} \approx \mathbf{0}$*. Therefore the transformation matrix between both type of stress resultants is approximately the identity matrix. Thus in case of small strains the numerical results of both formulations agree practically, which can also be seen from the examples in section 6.*

### *3.2 Linearization of the weak form of equilibrium*

For the subsequent finite element formulation we need to derive the linearization of the boundary value problem (13). This is formally achieved using the directional derivative

$$L[G(\mathbf{v},\delta\mathbf{v})] = G + \mathrm{D}G\cdot\Delta\mathbf{v} \qquad \mathrm{D}G\cdot\Delta\mathbf{v} = \frac{\mathrm{d}}{\mathrm{d}\varepsilon}[G(\mathbf{v}+\varepsilon\Delta\mathbf{v})]_{\varepsilon=0} \tag{29}$$

where $\Delta\mathbf{v} = [\Delta\mathbf{u}, \Delta\mathbf{w}]^T \in \mathcal{W}$ fulfils the boundary conditions on $\mathcal{S}_u$. First linearization of the internal virtual work leads to

$$\mathrm{D}G_{int}(\mathbf{v}, \delta\mathbf{v}) \cdot \Delta\mathbf{v} = \int_S (\delta\hat{\mathbf{E}}^T \mathbf{D} \Delta\hat{\mathbf{E}} + \Delta\delta\hat{\mathbf{E}}^T \hat{\mathbf{S}}) \, \mathrm{d}S \tag{30}$$

where $\mathbf{D} := \partial\hat{\mathbf{S}}/\partial\hat{\mathbf{E}}$ is specified for special constitutive behaviour in the next section. The linearized beam strains $\Delta\hat{\mathbf{E}} = [\Delta\varepsilon, \Delta\kappa_2, \Delta\kappa_3, \Delta\gamma_2, \Delta\gamma_3, \Delta\vartheta]^T$ can be expressed by

$$\Delta\hat{\mathbf{E}} = \mathbf{H} \, (\mathbf{L} \, \Delta\mathbf{v}) \, . \tag{31}$$

Next the geometric part of (30) is derived considering (22)

$$\int_S \Delta\delta\hat{\mathbf{E}}^T \hat{\mathbf{S}} \, \mathrm{d}S = \int_S (\mathbf{L} \, \delta\mathbf{v})^T \Delta\hat{\boldsymbol{\sigma}} \, \mathrm{d}S \, . \tag{32}$$

with $\Delta\hat{\boldsymbol{\sigma}} = \Delta\mathbf{H}^T \hat{\mathbf{S}}$ where the stress resultants $\hat{\mathbf{S}}$ are hold fixed. The linearization of the basis vectors $\mathbf{a}_i$ and associated derivatives read

$$\begin{aligned} \Delta\mathbf{a}_i &= \Delta\mathbf{w} \times \mathbf{a}_i = \mathbf{W}_i \, \Delta\mathbf{w} \\ \Delta\mathbf{a}_i' &= \Delta\mathbf{w} \times \mathbf{a}_i' + \Delta\mathbf{w}' \times \mathbf{a}_i \end{aligned} \tag{33}$$

which leads to

$$\Delta\hat{\boldsymbol{\sigma}} = \begin{bmatrix} \Delta\mathbf{f} \\ \mathbf{n} \times \Delta\mathbf{u}' + \Delta\mathbf{n} \times \mathbf{x}_0' \\ \Delta\mathbf{m} \end{bmatrix} = \begin{bmatrix} N\Delta\mathbf{u}' + \Delta\mathbf{w} \times \mathbf{n} + \Delta\mathbf{w}' \times \mathbf{l} \\ \mathbf{n} \times \Delta\mathbf{u}' + (\Delta\mathbf{w} \times \mathbf{n} + \Delta\mathbf{w}' \times \mathbf{l}) \times \mathbf{x}_0' \\ \Delta\mathbf{w} \times M^1\mathbf{a}_1 + \mathbf{l} \times \Delta\mathbf{u}' + (\Delta\mathbf{w} \times \mathbf{l}) \times \mathbf{x}_0' \end{bmatrix} .$$

Using the relation $(\mathbf{a} \times \mathbf{b}) \times \mathbf{c} = [\mathbf{b} \otimes \mathbf{c} - (\mathbf{b} \cdot \mathbf{c})\mathbf{1}] \, \mathbf{a}$ the tensors $\mathbf{A}_n$ and $\mathbf{A}_l$ are defined. Furthermore the skew–symmetric tensors $\mathbf{W}_n$ and $\mathbf{W}_l$ can be computed

$$\begin{aligned} \mathbf{A}_n &= \mathbf{n} \otimes \mathbf{x}_0' - (\mathbf{n} \cdot \mathbf{x}_0')\mathbf{1} & \mathbf{W}_n \, \mathbf{a} &= \mathbf{a} \times \mathbf{n} \qquad \forall \, \mathbf{a} \\ \mathbf{A}_l &= \mathbf{l} \otimes \mathbf{x}_0' - (\mathbf{l} \cdot \mathbf{x}_0')\mathbf{1} & \mathbf{W}_l \, \mathbf{a} &= \mathbf{a} \times \mathbf{l} \end{aligned} \tag{34}$$

and one obtains

$$\Delta\hat{\boldsymbol{\sigma}} = \begin{bmatrix} N\Delta\mathbf{u}' + \mathbf{W}_n\Delta\mathbf{w} + \mathbf{W}_l\Delta\mathbf{w}' \\ \mathbf{W}_n^T\Delta\mathbf{u}' + \mathbf{A}_n\Delta\mathbf{w} + \mathbf{A}_l\Delta\mathbf{w}' \\ \mathbf{W}_l^T\Delta\mathbf{u}' + (M^1\mathbf{W}_1 + \mathbf{A}_l)\Delta\mathbf{w} \end{bmatrix} . \tag{35}$$

The linearization of external virtual work (21) reads

$$\mathrm{D}G_{ext}(\mathbf{v},\delta\mathbf{v})\cdot\Delta\mathbf{v} = -\int_S \delta\mathbf{w}\cdot\Delta\hat{\mathbf{m}}\,\mathrm{d}S = \int_S \delta\mathbf{w}\cdot\hat{\mathbf{A}}\,\Delta\mathbf{w}\,\mathrm{d}S \tag{36}$$

with $\hat{\mathbf{A}} = -[\mathbf{d}\otimes\hat{\mathbf{p}} - (\mathbf{d}\cdot\hat{\mathbf{p}})\mathbf{1}]$. Above equations show that $\hat{\mathbf{m}}$ and $\hat{\mathbf{A}}$ vanish as the vector $\mathbf{d}$ goes to zero. This is the case when the loading acts on the reference curve.

Hence the final version of (29) reads

$$\begin{aligned}
\mathrm{D}G(\mathbf{v},\delta\mathbf{v})\cdot\Delta\mathbf{v} &= \int_S (\mathbf{L}\,\delta\mathbf{v})^T\,(\hat{\mathbf{D}}+\mathbf{G}+\hat{\mathbf{P}})\,(\mathbf{L}\,\Delta\mathbf{v})\,\mathrm{d}S \\
\hat{\mathbf{D}} = \mathbf{H}^T\mathbf{D}\mathbf{H}\,,\quad \mathbf{G} &= \begin{bmatrix} N\mathbf{1} & \mathbf{W}_n & \mathbf{W}_l \\ \mathbf{W}_n^T & \mathbf{A}_n & \mathbf{A}_l \\ \mathbf{W}_l^T & M^1\mathbf{W}_1+\mathbf{A}_l & \mathbf{0} \end{bmatrix}, \quad \hat{\mathbf{P}} = \begin{bmatrix} \mathbf{0} & \mathbf{0} & \mathbf{0} \\ \mathbf{0} & \hat{\mathbf{A}} & \mathbf{0} \\ \mathbf{0} & \mathbf{0} & \mathbf{0} \end{bmatrix}.
\end{aligned} \tag{37}$$

As can be seen, the material part $\hat{\mathbf{D}}$ is symmetric provided $\mathbf{D}$ is symmetric, whereas the geometric matrix $\mathbf{G}$ and the load stiffness matrix $\hat{\mathbf{P}}$ are non–symmetric.

The condition of conservative loading can be written as

$$\hat{\mathbf{m}}(S) = \mathbf{0} \qquad S\in[0,L] \qquad \text{and} \qquad [\mathbf{m}\cdot(\delta\boldsymbol{\omega}\times\Delta\boldsymbol{\omega})]_{S=0}^{L} = 0\,. \tag{38}$$

Since the variation $\delta\mathbf{v}\in\mathcal{V}$ has to be a kinematically admissible function the boundary term vanishes in view of (14) on boundaries with prescribed rotations. However the boundary term does not vanish for the case of an applied end moment with "fixed spatial axes", see Refs. [1,2]. In the following it is assumed that (38) holds.

Hence the geometric stiffness $\mathbf{G}$ becomes symmetric if the transformation

$$\delta\mathbf{w} = \mathbf{T}(\Delta\boldsymbol{\omega})\,\delta\boldsymbol{\omega} \tag{39}$$

is introduced.
The tensor $\mathbf{T}(\Delta\boldsymbol{\omega})$ can be chosen arbitrarily with $\mathbf{T}(\Delta\boldsymbol{\omega}=\mathbf{0})=\mathbf{1}$. Thus $\delta\mathbf{w}=\delta\boldsymbol{\omega}$ holds at an equilibrium configuration. The infinitesimal rotations $\delta\mathbf{w}$ are comparable with the semi–tangential rotations introduced by Argyris et.al. [1] – [3], [17]. Now the linearization of the internal virtual work (30) with respect to $\Delta\tilde{\mathbf{v}} = [\Delta\mathbf{u},\Delta\boldsymbol{\omega}]^T$ is rewritten. Considering (25), (38) and a special

choice of $\mathbf{T}(\Delta\boldsymbol{\omega})$ with $\Delta\delta\mathbf{w} = 1/2\Delta\boldsymbol{\omega} \times \delta\boldsymbol{\omega}$ one obtains

$$\begin{aligned} \mathrm{D}G_{int}(\mathbf{v}, \delta\mathbf{v}) \cdot \Delta\tilde{\mathbf{v}} = & \int_S (\mathbf{L}\,\delta\tilde{\mathbf{v}})^T (\hat{\mathbf{D}} + \mathbf{G})\,(\mathbf{L}\,\Delta\tilde{\mathbf{v}})\,\mathrm{d}S \\ & - \frac{1}{2}\int_S [(\mathbf{m}' + \mathbf{x}_0' \times \mathbf{f}) \cdot (\Delta\boldsymbol{\omega} \times \delta\boldsymbol{\omega})]\,\mathrm{d}S\,. \end{aligned} \tag{40}$$

The geometric matrix $\mathbf{G} = \mathbf{G}^S + \mathbf{G}^A$ is separated into the symmetric part $\mathbf{G}^S = 1/2(\mathbf{G} + \mathbf{G}^T)$ and the skew–symmetric part $\mathbf{G}^A = 1/2(\mathbf{G} - \mathbf{G}^T)$. Furthermore the skew–symmetric tensors and associated axial vectors are introduced

$$\begin{aligned} \mathbf{A}_n^A\,\Delta\boldsymbol{\omega} &= \frac{1}{2}(\mathbf{n} \otimes \mathbf{x}_0' - \mathbf{x}_0' \otimes \mathbf{n})\,\Delta\boldsymbol{\omega} \\ &= \frac{1}{2}(\mathbf{x}_0' \times \mathbf{n}) \times \Delta\boldsymbol{\omega} = \frac{1}{2}(\mathbf{x}_0' \times \mathbf{f}) \times \Delta\boldsymbol{\omega} \\ (\frac{1}{2}M^1\mathbf{W}_1 + \mathbf{A}_l^A)\,\Delta\boldsymbol{\omega} &= \frac{1}{2}(M^1\mathbf{W}_1 + \mathbf{l} \otimes \mathbf{x}_0' - \mathbf{x}_0' \otimes \mathbf{l})\,\Delta\boldsymbol{\omega} \\ &= -\frac{1}{2}(M^1\mathbf{a}_1 + \mathbf{l} \times \mathbf{x}_0') \times \Delta\boldsymbol{\omega} = -\frac{1}{2}\mathbf{m} \times\ \Delta\boldsymbol{\omega}\,. \end{aligned} \tag{41}$$

Integration by parts and further reformulation using (41) is applied to the second integral of (40)

$$\begin{aligned} & -\frac{1}{2}\int_S [\boldsymbol{m} \cdot (\delta\boldsymbol{\omega} \times \Delta\boldsymbol{\omega})' - (\mathbf{x}_0' \times \mathbf{f}) \cdot (\delta\boldsymbol{\omega} \times \Delta\boldsymbol{\omega})]\,\mathrm{d}S \\ = & -\frac{1}{2}\int_S \{\delta\boldsymbol{\omega} \cdot [(\mathbf{x}_0' \times \mathbf{f}) \times \Delta\boldsymbol{\omega}] - \delta\boldsymbol{\omega} \cdot (\mathbf{m} \times \Delta\boldsymbol{\omega}') - \delta\boldsymbol{\omega}' \cdot (\mathbf{m} \times \Delta\boldsymbol{\omega})\}\,\mathrm{d}S \\ = & -\int_S \delta\boldsymbol{\omega} \cdot [\mathbf{A}_n^A\Delta\boldsymbol{\omega} + (\frac{1}{2}M^1\mathbf{W}_1 + \mathbf{A}_l^A)\,\Delta\boldsymbol{\omega}'] + \delta\boldsymbol{\omega}' \cdot (\frac{1}{2}M^1\mathbf{W}_1 + \mathbf{A}_l^A)\,\Delta\boldsymbol{\omega}]\,\mathrm{d}S \\ = & -\int_S (\mathbf{L}\,\delta\tilde{\mathbf{v}})^T\,\mathbf{G}^A\,(\mathbf{L}\,\Delta\tilde{\mathbf{v}})\,\mathrm{d}S \end{aligned}$$

which shows that the skew–symmetric part of $\mathbf{G}$ in (40) cancels out.

Next the linearization of the external virtual work (36) is rewritten considering

the metric (39)

$$\begin{aligned} \mathrm{D}G_{ext}(\mathbf{v},\delta\mathbf{v})\cdot\Delta\tilde{\mathbf{v}} &= -\int_S [\delta\boldsymbol{\omega}\cdot\Delta\hat{\mathbf{m}} + \frac{1}{2}\hat{\mathbf{m}}\cdot(\Delta\boldsymbol{\omega}\times\delta\boldsymbol{\omega})]\,\mathrm{d}S \\ &= -\int_S \delta\boldsymbol{\omega}\cdot[\Delta\hat{\mathbf{m}} + \frac{1}{2}(\mathbf{d}\times\hat{\mathbf{p}})\times\Delta\boldsymbol{\omega}]\,\mathrm{d}S \\ &= \int_S \delta\boldsymbol{\omega}\cdot[\hat{\mathbf{A}} - \frac{1}{2}(\hat{\mathbf{p}}\otimes\mathbf{d} - \mathbf{d}\otimes\hat{\mathbf{p}})]\Delta\boldsymbol{\omega}\,\mathrm{d}S \\ &= \int_S \delta\boldsymbol{\omega}\cdot\hat{\mathbf{A}}^S\,\Delta\boldsymbol{\omega}\,\mathrm{d}S \end{aligned} \tag{42}$$

with $\hat{\mathbf{A}}^S = \frac{1}{2}(\hat{\mathbf{A}} + \hat{\mathbf{A}}^T)$. This shows that an external loading according to (20) results into a symmetric load stiffness.

We conclude that for conservative loading the linearization leads to a symmetric bilinear form with respect to a special transformation (39)

$$\mathrm{D}G(\mathbf{v},\delta\mathbf{v})\cdot\Delta\tilde{\mathbf{v}} = \int_S (\mathbf{L}\,\delta\tilde{\mathbf{v}})^T(\hat{\mathbf{D}} + \mathbf{G}^S + \hat{\mathbf{P}}^S)\,(\mathbf{L}\,\Delta\tilde{\mathbf{v}})\,\mathrm{d}S\,. \tag{43}$$

Furthermore, provided the loading is conservative, one can show that the skew–symmetric part of (37) cancels out at an equilibrium configuration for any $\mathbf{T}(\Delta\boldsymbol{\omega})$, see also [21].

## 4 Linear Elastic Material Law

In this section we introduce the so–called Saint–Venant–Kirchhoff material where a linear isotropic relation between $\mathbf{S}$ and $\mathbf{E}$ is postulated, see e.g. [22]. Since the stress components $S^{22}, S^{33}, S^{23}$ are assumed to be zero, the nonvanishing components are obtained by

$$S^{11} = E\,E_{11}\,, \qquad S^{12} = 2\,G\,E_{12}\,, \qquad S^{13} = 2\,G\,E_{13}\,, \tag{44}$$

where $E$ and $G$ denote Young's modulus and shear modulus, respectively. With these constitutive equations we are restricted to linear elastic material with small strains. The constitutive relations for the stress resultants (16) can

easily be derived using (12) as follows

$$\begin{bmatrix} N \\ M^2 \\ M^3 \\ Q^2 \\ Q^3 \\ M^1 \end{bmatrix} = \int_A \begin{bmatrix} E & E\xi_3 & E\xi_2 & 0 & 0 & 0 \\ E\xi_3 & E\xi_3^2 & E\xi_2\xi_3 & 0 & 0 & 0 \\ E\xi_2 & E\xi_2\xi_3 & E\xi_2^2 & 0 & 0 & 0 \\ 0 & 0 & 0 & G & 0 & -G\tilde{\xi}_3 \\ 0 & 0 & 0 & 0 & G & G\tilde{\xi}_2 \\ 0 & 0 & 0 & -G\tilde{\xi}_3 & G\tilde{\xi}_2 & G(\tilde{\xi}_2^2+\tilde{\xi}_3^2) \end{bmatrix} \mathrm{d}A \begin{bmatrix} \varepsilon \\ \kappa_2 \\ \kappa_3 \\ \gamma_2 \\ \gamma_3 \\ \vartheta \end{bmatrix} \qquad (45)$$

$$\hat{\mathbf{S}} = \mathbf{D}\hat{\mathbf{E}}$$

The centroid of the cross–section with coordinates $\{s_2, s_3\}$ is denoted by $S$, see Fig. 1. Furthermore we denote the area of the cross–section by $A$, the moments of inertia relative to the centroid by $I_{22}, I_{33}, I_{23}$ and the Saint–Venant torsion modulus by $I_T$ and introduce the following definitions

$$\begin{aligned} S_\alpha &:= \int_A \xi_\alpha \mathrm{d}A = A s_\alpha && (\alpha = 2,3) \\ \tilde{I}_{\alpha\beta} &:= \int_A \xi_\alpha \xi_\beta \, \mathrm{d}A = I_{\alpha\beta} + A s_\alpha s_\beta && (\alpha,\beta = 2,3) \\ I_T &:= \int_A \left[(\xi_2 - m_2)^2 + (\xi_3 - m_3)^2 + \tilde{w}_{,3}\,(\xi_2 - m_2) - \tilde{w}_{,2}\,(\xi_3 - m_3)\right] \mathrm{d}A\,. \end{aligned} \qquad (46)$$

Using the equations of Saint–Venants torsion theory (4) and application of Green's theorem yields after some algebra the missing quantities, see appendix A.3

$$\begin{aligned} M_\alpha &:= \int_A \tilde{\xi}_\alpha \, \mathrm{d}A = A m_\alpha && (\alpha = 2,3) \\ \tilde{I}_T &:= \int_A (\tilde{\xi}_2^2 + \tilde{\xi}_3^2) \, \mathrm{d}A = I_T + A(m_2^2 + m_3^2)\,. \end{aligned} \qquad (47)$$

Hence with (46) and (47) the elasticity matrix is expressed in terms of section quantities in the following form

$$\mathbf{D} = \begin{bmatrix} EA & EAs_3 & EAs_2 & 0 & 0 & 0 \\ EAs_3 & E\tilde{I}_{22} & E\tilde{I}_{23} & 0 & 0 & 0 \\ EAs_2 & E\tilde{I}_{23} & E\tilde{I}_{33} & 0 & 0 & 0 \\ 0 & 0 & 0 & GA & 0 & -GAm_3 \\ 0 & 0 & 0 & 0 & GA & GAm_2 \\ 0 & 0 & 0 & -GAm_3 & GAm_2 & G\tilde{I}_T \end{bmatrix} . \tag{48}$$

We note that the elasticity matrix is constant and symmetric. As can be seen torsion–bending coupling occurs if the reference point $O$ and the shear center $M$ with coordinates $\{m_2, m_3\}$ do not coincide. If the coordinates $\{\xi_2, \xi_3\}$ define principal axes of the cross–section and if $S = M = O$ one obtains the well–known diagonal matrix $\mathbf{D} = \text{diag}\,[EA, EI_{22}, EI_{33}, GA, GA, GI_T]$ .

## 5 Finite Element Approximation

In this section we describe the finite element approximation associated with the continuum weak form (22). According to the isoparametric concept, the following kinematic variables are interpolated with standard Lagrangean shape functions $N_I(\xi)$, e.g. see [23]. The normalized coordinate is defined in the range $-1 \leq \xi \leq +1$. Within an element the position vector of the reference curve $\mathcal{S}_0^h$ and the curve $\mathcal{S}^h$ of the current configuration are interpolated by

$$\mathbf{X}_0^h = \sum_{I=1}^{nel} N_I(\xi)\mathbf{X}_I \,, \qquad \mathbf{x}_0^h = \sum_{I=1}^{nel} N_I(\xi)(\mathbf{X}_I + \mathbf{u}_I) \,. \tag{49}$$

Here $nel$ denotes the number of nodes at the element. For $nel \geq 3$ the reference curve of a space–curved beam is approximated by polynomial functions.

The derivative of the shape functions $N_I(\xi)$ with respect to the arc–length parameter $S$ can now be expressed using the chain rule $N_I'(\xi) = N_I(\xi)_{,\xi} \; / |\mathbf{X}_{0,\xi}^h|$. Introducing the matrix $\mathbf{B}_I$ which contains the shape functions $N_I$ and the derivatives $N_I'$

$$\mathbf{B}_I = \begin{bmatrix} N_I'\mathbf{1} & \mathbf{0} \\ \mathbf{0} & N_I\mathbf{1} \\ \mathbf{0} & N_I'\mathbf{1} \end{bmatrix} \tag{50}$$

the variation $\delta\mathbf{v}^h \in \mathcal{V}^h$ and the linearization $\Delta\mathbf{v}^h \in \mathcal{W}^h$ follow from the finite element approximation

$$\mathbf{L}\,\delta\mathbf{v}^h = \sum_{I=1}^{nel} \mathbf{B}_I\,\delta\mathbf{v}_I \qquad\qquad \mathbf{L}\,\Delta\mathbf{v}^h = \sum_{K=1}^{nel} \mathbf{B}_K\,\Delta\mathbf{v}_K\,. \tag{51}$$

where $\delta\mathbf{v}_I = [\delta\mathbf{u}_I, \delta\boldsymbol{\omega}_I]^T$ and $\Delta\mathbf{v}_K = [\Delta\mathbf{u}_K, \Delta\boldsymbol{\omega}_K]^T$. The tangential vectors $\mathbf{X}_0'$ and $\mathbf{x}_0'$ are given replacing $N_I$ by $N_I'$ in (49). Furthermore the basis vectors $\mathbf{a}_i$ and the associated derivatives $\mathbf{a}_i'$ are obtained within the multiplicative update procedure according to appendix A.1.

The finite element interpolation (51) is inserted into the linearized boundary value problem (29)

$$L[G(\mathbf{v}^h, \delta\mathbf{v}^h)] = \mathop{\mathsf{A}}_{e=1}^{numel} \sum_{I=1}^{nel}\sum_{K=1}^{nel} \delta\mathbf{v}_I^T\,(\mathbf{f}_I^e + \mathbf{K}_{IK}^e \Delta\mathbf{v}_K)\,. \tag{52}$$

where $\mathsf{A}$ denotes the standard assembly operator and *numel* the total number of elements to discretize the problem. Furthermore $\mathbf{f}_I^e$ and $\mathbf{K}_{IK}^e$ denote the sum of the internal and external nodal forces of node $I$ and the tangential stiffness matrix of element $e$ related to nodes $I$ and $K$, respectively. Considering (22) and (37) one obtains

$$\begin{aligned} \mathbf{f}_I^e &= \int_S \mathbf{B}_I^T \hat{\boldsymbol{\sigma}}^h\,\mathrm{d}S - \int_S N_I\,\hat{\mathbf{q}}^h\,\mathrm{d}S \\ \mathbf{K}_{IK}^e &= \int_S \mathbf{B}_I^T\,(\hat{\mathbf{D}} + \mathbf{G} + \hat{\mathbf{P}})\,\mathbf{B}_K\,\mathrm{d}S\,. \end{aligned} \tag{53}$$

The stress resultants $\hat{\mathbf{S}}^h$ follow from the material law (45) and are summarized in the vector $\hat{\boldsymbol{\sigma}}^h = \mathbf{H}^T\,\hat{\mathbf{S}}^h$ according to $(23)_1$. The loading is approximated by $\hat{\mathbf{p}}^h(S) = \sum_I^{nel} N_I(\xi)\hat{\mathbf{p}}_I$ which yields the vector $\hat{\mathbf{q}}^h$ according to $(23)_2$. In case of conservative loading the matrices $\mathbf{G}$ and $\hat{\mathbf{P}}$ can be replaced by its symmetric part, see eq. (43).

Application of the chain rule yields the differential arc–length $\mathrm{d}S = |\mathbf{X}_{0,\xi}^h|\,\mathrm{d}\xi$. The integration of the element residual and element stiffness matrix (53) with respect to the coordinate $S$ is performed numerically. To avoid locking effects uniform reduced integration is applied to all quantities. Eq. (52) leads to a linear system of equations for the incremental nodal degrees of freedom. Hence the equilibrium configuration is computed iteratively within the Newton iteration procedure.

## 6 Numerical examples

The element scheme has been implemented in an enhanced version of the program FEAP documented in [23]. In this section several nonlinear examples with large deformations are presented. The first two examples are taken from the literature. The third example is concerned with a cross–section where the centroid, center of shear and loading point are not identical, thus bending and torsion coupling occurs. Within the last example a coupled beam–shell problem is solved. If possible comparisons with available solutions from the literature are given.

### *6.1 Right angle frame under applied end moments*

Our first example is a hinged right–angle frame first introduced by Argyris [2] and later analyzed by several other authors, e.g. [9,7]. The geometry and boundary conditions are illustrated in Fig. 2. Since the width to thickness ratio is 50 the cross–section is very slender, thus provides a severe test for the element formulation. At the support translation along x and rotation about z is permitted. At this point a moment about z is applied. The solution obtained with 10 three–noded beam elements for half the system is depicted in Fig. 3.

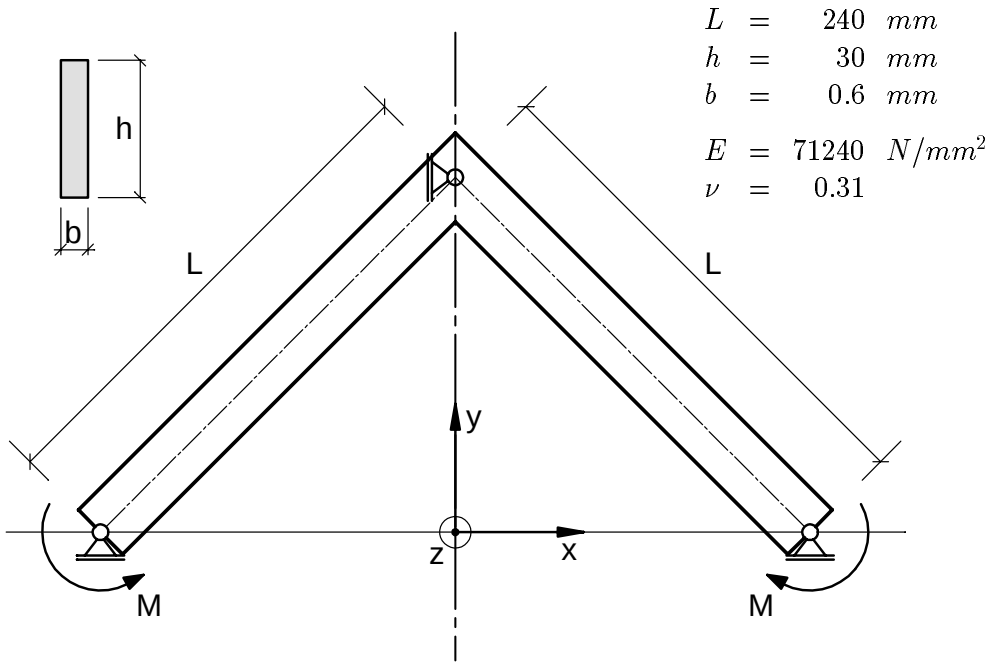


Fig. 2. Right angle frame under applied end moments

A primary path represents the two–dimensional response in the x–y plane. A

bifurcation point is found at a load level of $622.7 Nmm$. A switch to the secondary path is possible by a perturbation of the primary solution with the first eigenvector. The secondary path exhibits the full three–dimensional response with two complete revolutions. One has to apply the arc–length–method to compute the entire load deflection curve according to Fig. 3. Although the reference solution [9] is based on different strain measures there is practically complete agreement. Table 1 shows a comparison of the residual norm and the energy norm computed from the symmetric and the non–symmetric tangent stiffness matrix at a displacement step from $60 \leq u_z \leq 62\, mm$. Since both versions are obtained by linearization of the weak form of equilibrium quadratic convergence is given in both cases. A sequence of deformed meshes is plotted in a perspective view in Fig. 4, where the rotation $\varphi_z$ of the loading point is parameter of the different configurations.

Table 1
Residual norm and energy norm computed from the symmetric and non–symmetric stiffness matrix

| Symmetric | | Non–symmetric | |
|---|---|---|---|
| Residual norm | Energy norm | Residual norm | Energy norm |
| 2.5280E+03 | 1.9640E+04 | 2.5280E+03 | 1.9640E+04 |
| 2.1283E+03 | 4.2304E+00 | 2.1282E+03 | 4.2307E+00 |
| 3.9302E+00 | 8.3562E–01 | 1.2138E+00 | 1.9723E–01 |
| 3.9407E+00 | 1.4288E–05 | 7.4304E–01 | 1.4490E–06 |
| 1.9704E+00 | 3.6367E–06 | 3.7152E–01 | 3.6258E–07 |
| 1.5563E–04 | 7.1588E–11 | 6.3715E–06 | 2.7374E–13 |
| 3.8042E–08 | 1.7320E–21 | 2.2713E–08 | 3.9757E–22 |

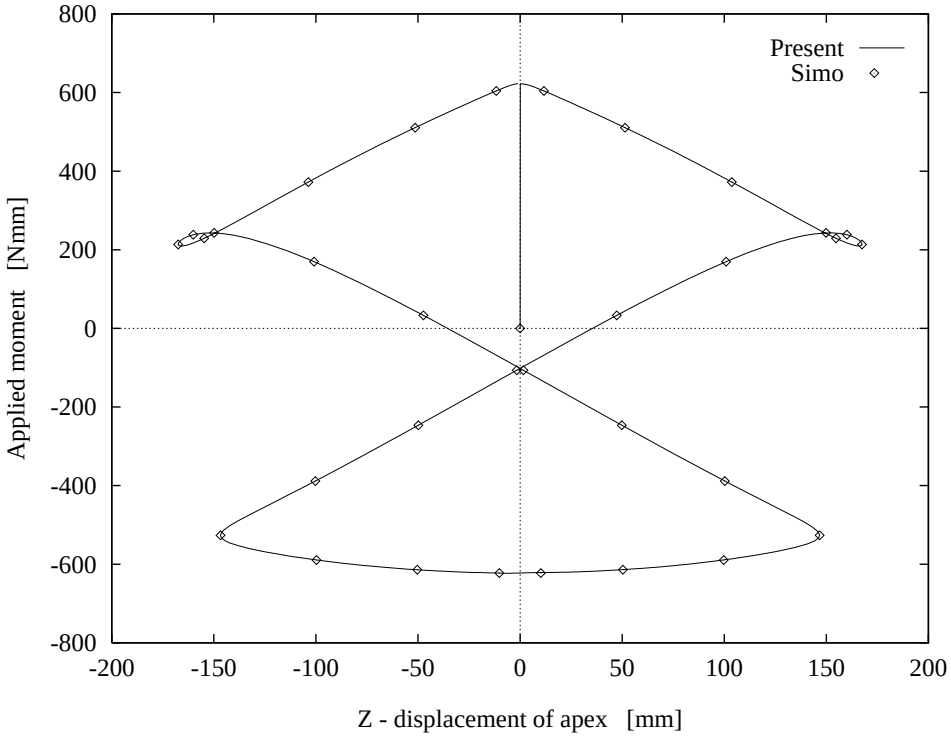


Fig. 3. Applied moment versus z–displacement of the apex of the frame

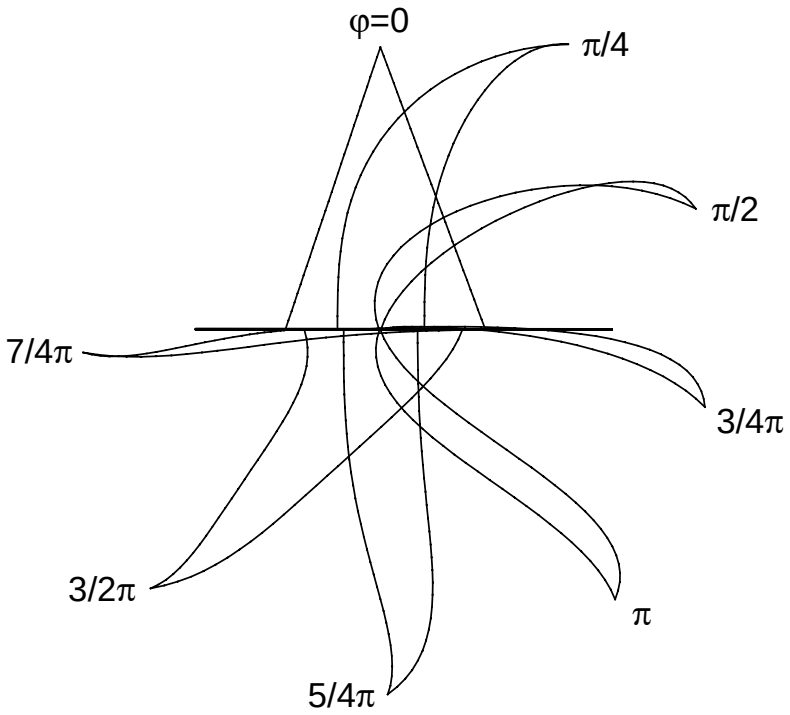


Fig. 4. Sequence of deformed configurations

### *6.2 Hockling problem of a cable under torsion*

In Fig. 5 a cable segment with associated geometrical and material data is depicted. The boundary conditions are as follows: at $x = 0$ all displacements and rotations are restrained and at $x = l$ only translation along $x$ and rotation about $x$ is permitted. The discretization is performed with 20 two–noded beam elements. The torque applied to the cable is increased up to a critical value of 225.4 $Nmm$. Here bifurcation to a secondary path which is characterized by a lower energy mode is possible.

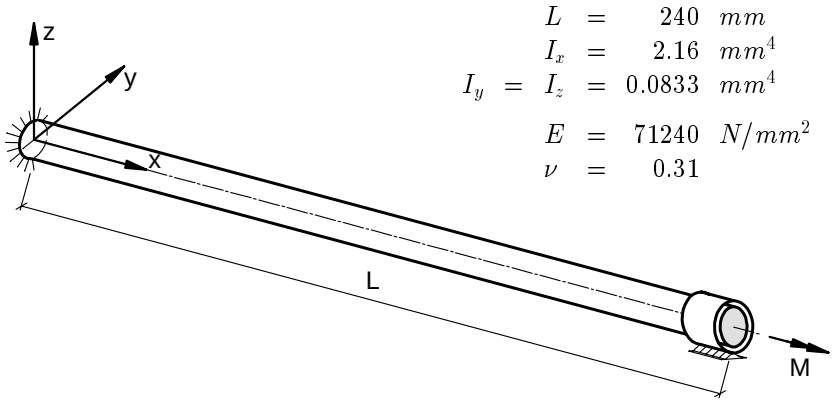


Fig. 5. Cable segment under torsion

The results of our calculation are depicted in Fig. 6. As can be seen there is complete agreement with the reference solution in [7]. A sequence of deformed configurations of the cable with rotational parameter $\varphi_x$ of the loading point is plotted in Fig. 7.

### *6.3 Channel–section beam*

A channel–section beam clamped at one end and subjected to a tip force at the free end is investigated next. Fig. 8 contains the problem description with geometrical and material data. The load is applied at the top of the web. The discretization is performed with 20 two–noded beam elements and in the second case with 180 four–noded shell elements, see Ref. [16]. For the shell discretization the mesh consists of 18 elements along the length direction, 6 elements along the web and 2 elements for each flange. In the following the vertical displacement $w$ of point $O$ at the cantilever tip is computed. We obtain a linear solution $w = 1.48\,cm$ with the beam discretization and $w = 1.47\,cm$ with the shell discretization at $P = 1\,kN$. Furthermore the nonlinear response is computed up to $P = 20\,kN$. The results for both models agree good in wide

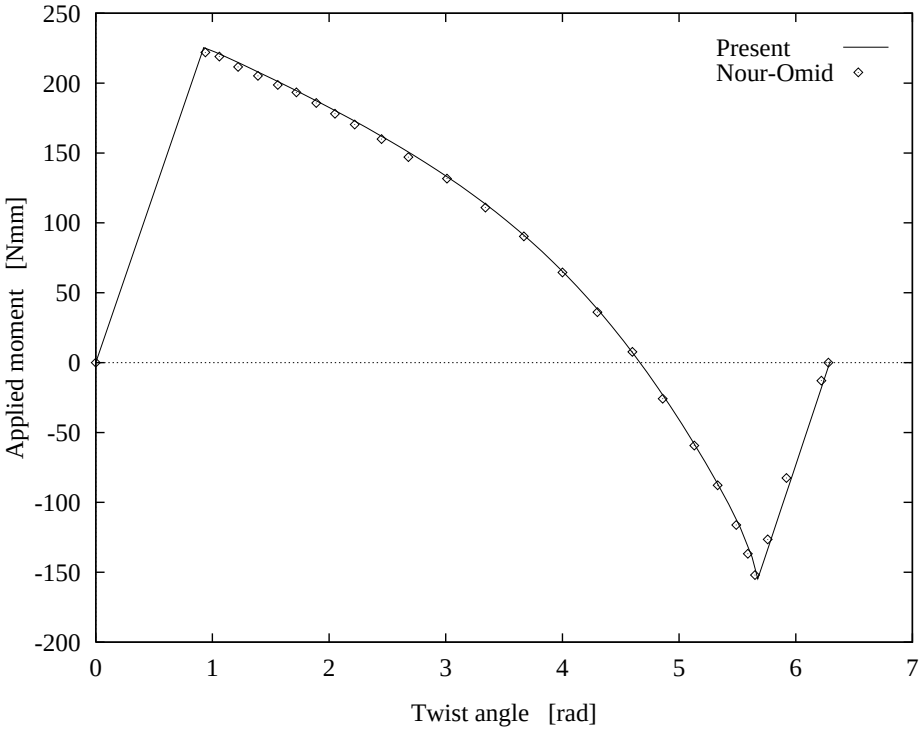


Fig. 6. Applied torque versus twist angle

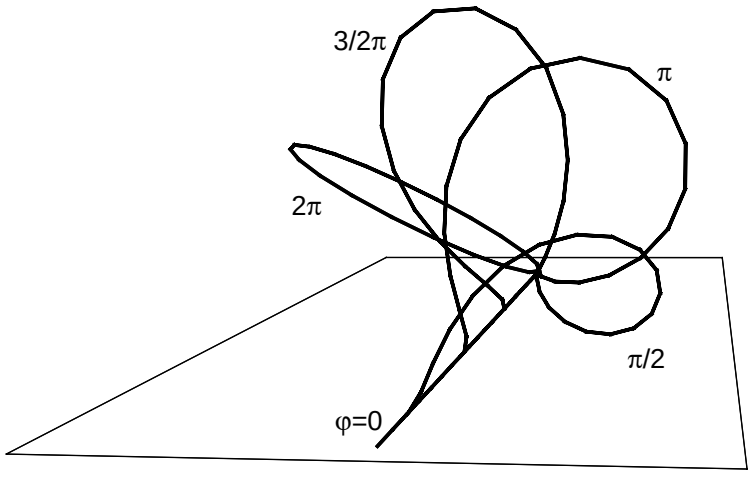


Fig. 7. Deformed configurations of the cable for different loads

ranges of the computed load deflection curve, see Fig. 9. Finally Fig. 10 shows the undeformed mesh and the configuration at $P = 9\,kN$.

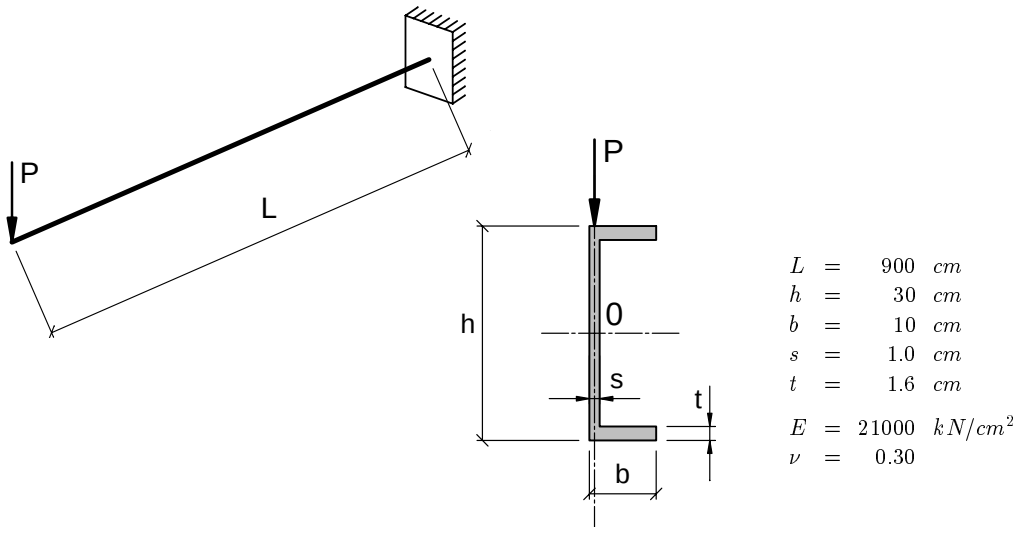


Fig. 8. Channel–section beam with geometrical and material data

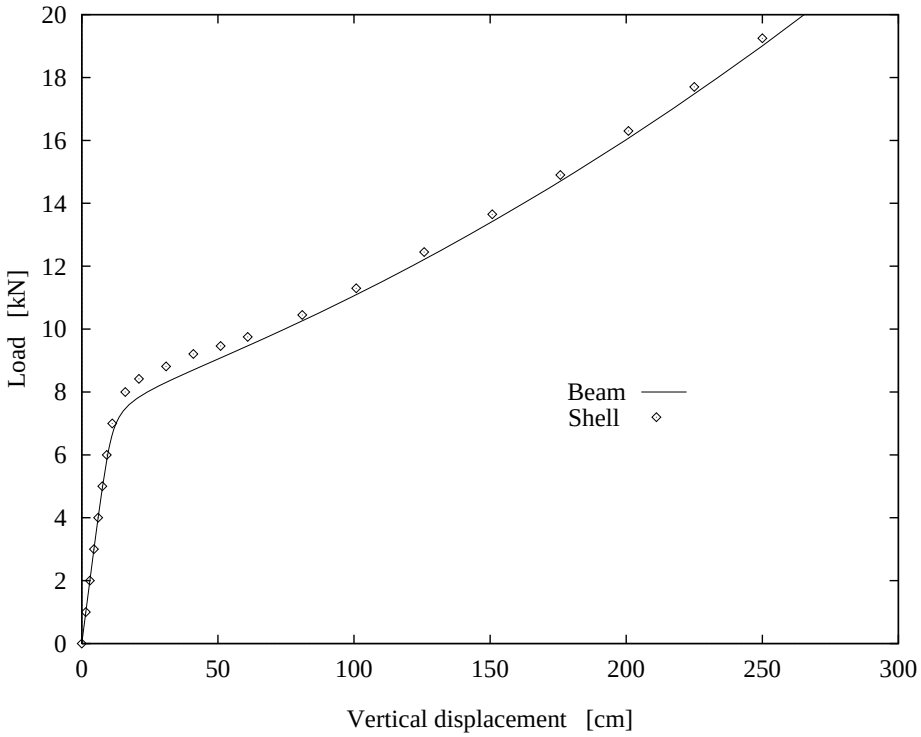


Fig. 9. Load deflection curves of the channel–section beam

### *6.4 Stiffened plate*

The main goal of this paper is the development of a beam element which can be used to discretize eccentric stiffeners of thin–walled structures. Therefore in this example the coupling of the beam with shell elements is investigated. Fig.

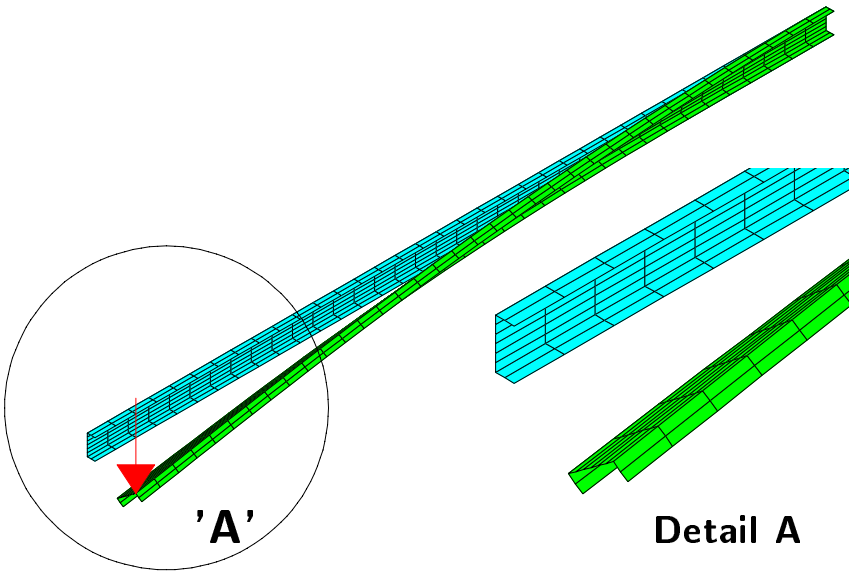


Fig. 10. Undeformed and deformed channel–section beam at $P = 9\,kN$

Table 2
Vertical displacement $w$ for P = 0.1 kN (linear solution)

| discretization | L 2.0 × 2.0 × 0.3 | L 5.0 × 4.0 × 0.5 |
|---|---|---|
| shell – shell | 12.094 cm | 2.417 cm |
| shell – beam | 11.976 cm | 2.410 cm |

11 shows the cross–section of a plate with two types of stiffeners. Furthermore the loading and the material data are given. The length and width of the plate are $L = 300\,cm$ and $b = 80\,cm$, respectively. The linear and nonlinear solutions are computed using two types of different discretizations. In both cases the plate is modeled using 20 four–noded shell elements in length direction and 10 elements in transverse direction. In the first case the L– shaped beam is discretized with 20 shell elements in length direction, 3 elements for the vertical leg and 2 elements for the horizontal leg. In the second case 20 two–noded beam elements are used. The vertical displacement of the loading point is computed for various load levels. First the linear solution is given in Table 2 for the shell–shell and the shell–beam discretization. The vertical displacement of the plate without stiffener is $w = 51.73\,cm$. Thus the stiffener leads to a significant reduction of the deformation. The nonlinear results are plotted in Fig. 12. For the thick stiffener the results agree practically up to $w \approx 75\,cm$. Furthermore there is almost complete agreement of the computed load deflection curve of the thin stiffener. The undeformed and deformed structures are depicted in Fig. 13. It can be seen that large deformations occur.

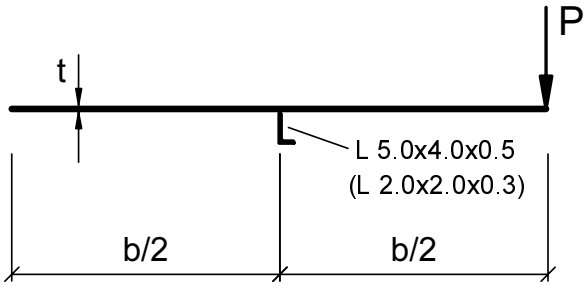


$$
\begin{aligned}
L &= 300 \ cm \\
b &= 80 \ cm \\
t &= 0.5 \ cm \\
E &= 21000 \ kN/cm^2 \\
\nu &= 0.30
\end{aligned}
$$

Fig. 11. Stiffened plate, problem description

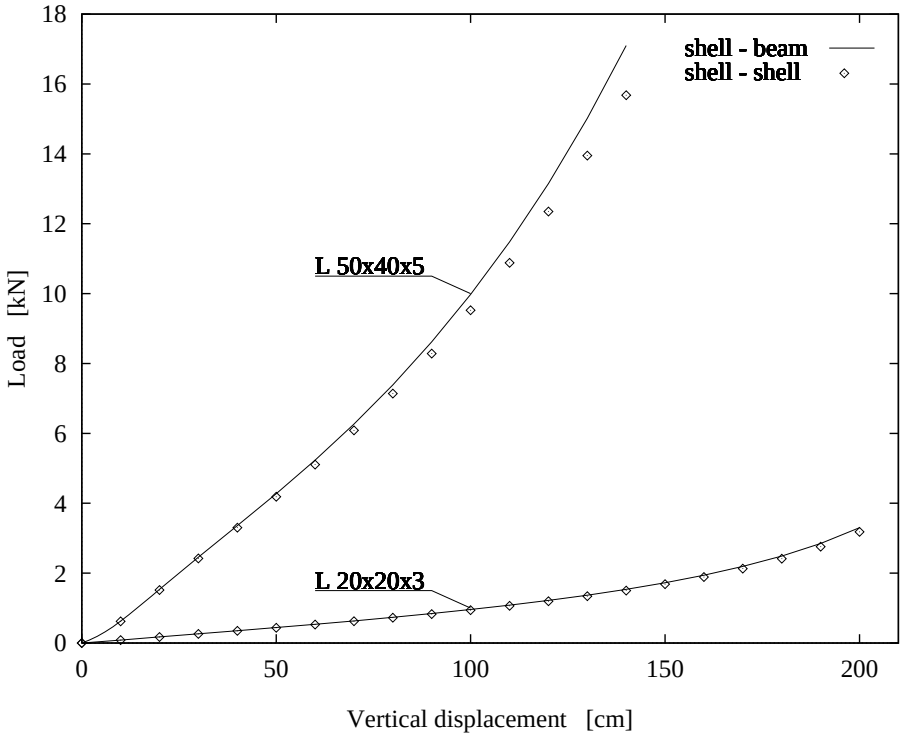


Fig. 12. Load deflection curves of the stiffened plate

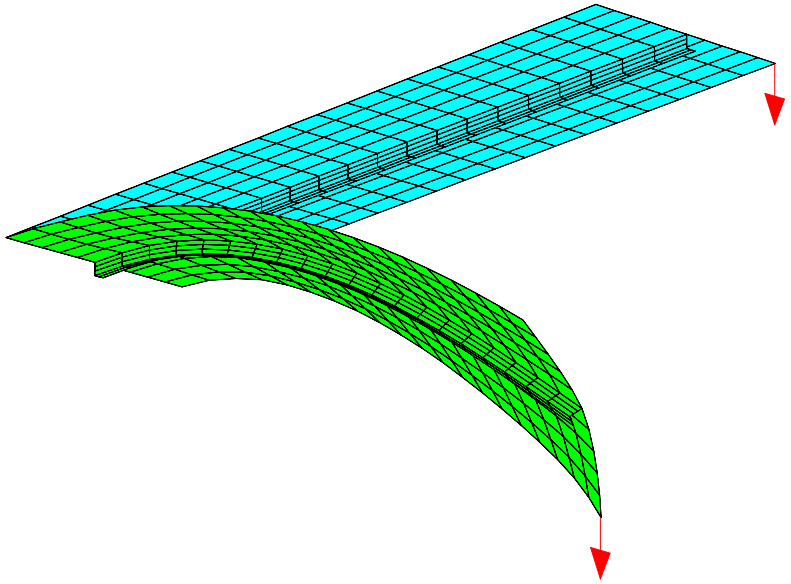

Fig. 13. Plot of the deformed stiffened plate with a shell discretization

## 7 Conclusions

In this paper the finite element formulation of a three–dimensional beam with arbitrary cross sections is developed. The arbitrary case is characterized by the fact that centroid and shear center do not coincide and torsion bending coupling occurs. Hence the kinematic assumption includes warping of the cross–sections. The beam strains are derived from the Green–Lagrangean strain tensor. Using additional constraints the kinematics can be described by six parameters. This leads to good numerical results if the so–called bi–moment does not play a significant role. Integrals of the warping function are reformulated using Green's formula and the equations of Saint–Venant torsion theory which leads to quantities of the cross–section. The resulting constitutive equation in terms of stress resultants yields a matrix representation where coupling of the shear forces with the torsion moment occurs. A comparison of the weak formulation with other stress resultants and work conjugate strains is presented. The derived linearized boundary value problem leads to a symmetric tangent operator for conservative loading.

The developed finite element model is fully consistent with existing six–parameter shell elements. Due to the arbitrary reference curve it can be used to model eccentric stiffener of shells. The computed results agree with available solutions from the literature. Further comparisons are given, where the beams are discretized with shell elements. Here also good agreement between the different models can be shown in large ranges of the computed load–deflection curves.

## A Appendix

### *A.1 Rotation tensor and derivatives*

In this appendix the orthogonal transformation (2) is specified. Here we adopt the multiplicative update procedure within the Newton iteration process as has been proposed for shells in Ref. [24]

$$\mathbf{a}_i^{(n+1)} = \Delta\mathbf{R}\,\mathbf{a}_i^{(n)} \qquad \text{with} \quad \mathbf{a}_i^{(0)} = \mathbf{A}_i \tag{A.1}$$

where $n$ denotes the iteration index. Hence $\Delta\mathbf{R}$ can be expressed as

$$\Delta\mathbf{R} = \mathbf{1} + c\,\Delta\boldsymbol{\Omega} + \frac{c}{2}\,\Delta\boldsymbol{\Omega}^2 \qquad c = (1 + \frac{\Delta\omega^2}{4})^{-1} \tag{A.2}$$

with $\Delta\omega = |\Delta\boldsymbol{\omega}|$ and the skew–symmetric tensor $\Delta\boldsymbol{\Omega}$ defined by $\Delta\boldsymbol{\Omega}\mathbf{a} = \Delta\boldsymbol{\omega} \times \mathbf{a} \quad \forall \mathbf{a}$.

From this equation, it is clear that $\Delta\mathbf{R}$ reduces to the identity tensor as the incremental axial vector $\Delta\boldsymbol{\omega}$ goes to zero. One can easily verify that $\Delta\mathbf{R}$ fulfills the orthogonality condition $\Delta\mathbf{R}^T\Delta\mathbf{R} = \mathbf{1}$. Furthermore we emphasize that (A.2) does not require any trigonometric functions. However it should be noted that above representation of the rotation tensor has to be used within a multiplicative update procedure, since it provides an approximation for finite rotations.

The derivative of the basis vectors $\mathbf{a}_i$ with respect to the arc–length $S$ yields

$$\begin{aligned} \mathbf{a}_i'^{(n+1)} &= \Delta\mathbf{R}'\,\mathbf{a}_i^{(n)} + \Delta\mathbf{R}\,\mathbf{a}_i'^{(n)} \\ &= \Delta\mathbf{R}'\Delta\mathbf{R}^T\mathbf{a}_i^{(n+1)} + \Delta\mathbf{R}\,\mathbf{a}_i'^{(n)} \\ &= \Delta\boldsymbol{\theta} \times \mathbf{a}_i^{(n+1)} + \Delta\mathbf{R}\,\mathbf{a}_i'^{(n)} \end{aligned} \tag{A.3}$$

The derivative of $\Delta\mathbf{R}$ follows from (A.2)

$$\Delta\mathbf{R}' \;=\; c'\,\Delta\boldsymbol{\Omega} \;+\frac{c'}{2}\Delta\boldsymbol{\Omega}^2 \;+c\,\Delta\boldsymbol{\Omega}' \;+\frac{c}{2}(\Delta\boldsymbol{\Omega}'\Delta\boldsymbol{\Omega} + \Delta\boldsymbol{\Omega}\Delta\boldsymbol{\Omega}') \tag{A.4}$$

where $c' = -c^2(\Delta\boldsymbol{\omega}' \cdot \Delta\boldsymbol{\omega})/2$ .

Using the following relations, see e.g. Argyris [17]

$$\begin{aligned} \Delta\boldsymbol{\Omega}^2 &= \Delta\boldsymbol{\omega} \otimes \Delta\boldsymbol{\omega} - \Delta\omega^2\mathbf{1} & \Delta\boldsymbol{\Omega}'\Delta\boldsymbol{\Omega} &= \Delta\boldsymbol{\omega} \otimes \Delta\boldsymbol{\omega}' - (\Delta\boldsymbol{\omega} \cdot \Delta\boldsymbol{\omega}')\,\mathbf{1} \\ \Delta\boldsymbol{\Omega}^3 &= -\Delta\omega^2\,\Delta\boldsymbol{\Omega} & \Delta\boldsymbol{\Omega}\Delta\boldsymbol{\Omega}'\Delta\boldsymbol{\Omega} &= -(\Delta\boldsymbol{\omega} \cdot \Delta\boldsymbol{\omega}')\,\Delta\boldsymbol{\Omega} \end{aligned} \tag{A.5}$$

one obtains after some algebra

$$\Delta\mathbf{R}'\,\Delta\mathbf{R}^T \;=\; c\,\Delta\boldsymbol{\Omega}' + \frac{c}{2}\,(\Delta\boldsymbol{\omega}' \otimes \Delta\boldsymbol{\omega} - \Delta\boldsymbol{\omega} \otimes \Delta\boldsymbol{\omega}') \tag{A.6}$$

and the associated axial vector

$$\Delta\boldsymbol{\theta} \;=\; c\,(\mathbf{1} + \frac{1}{2}\Delta\boldsymbol{\Omega})\,\Delta\boldsymbol{\omega}'\,. \tag{A.7}$$

### *A.2 Proof of relation (18)$_3$*

Since the sequence of variation and partial derivative can be exchanged the following relation holds

$$(\delta\mathbf{a}_i)' \;=\; \delta(\mathbf{a}_i')\,. \tag{A.8}$$

Using (3) and $(18)_1$ one obtains

$$\delta\mathbf{w}' \times \mathbf{a}_i + \delta\mathbf{w} \times (\boldsymbol{\theta} \times \mathbf{a}_i) \;=\; \delta\boldsymbol{\theta} \times \mathbf{a}_i + \boldsymbol{\theta} \times (\delta\mathbf{w} \times \mathbf{a}_i)\,. \tag{A.9}$$

Application of the Lagrangean identity for double vector products leads to

$$(\delta\mathbf{w}' - \delta\boldsymbol{\theta} + \delta\mathbf{w} \times \boldsymbol{\theta}) \times \mathbf{a}_i \;=\; \mathbf{0}\,. \tag{A.10}$$

Equation (A.10) only holds for arbitrary $\mathbf{a}_i$ if the term in brackets vanishes which proofs $(18)_3$ .

### *A.3 Proof of integrals (47)*

Using $(4)_1$ the following integral is reformulated such that Green's formula can be applied

$$\int\limits_A \tilde{w}_{,2}\;\mathrm{d}A \;=\; \int\limits_A \left[(\xi_2\tilde{w}_{,2}\,)_{,2} + (\xi_2\tilde{w}_{,3}\,)_{,3}\,\right]\mathrm{d}A \;=\; \oint\limits_C \left[\xi_2(\tilde{w}_{,2}\,n_2 + \tilde{w}_{,3}\,n_3)\right]\mathrm{d}C \tag{A.11}$$

Then inserting boundary condition $(4)_2$ yields

$$\oint\limits_C \left[\xi_2(\tilde{w}_{,2}\,n_2 + \tilde{w}_{,3}\,n_3)\right]\mathrm{d}C \;=\; \oint\limits_C \left[\xi_2(\xi_3 - m_3)n_2 - \xi_2(\xi_2 - m_2)n_3\right]\mathrm{d}C \tag{A.12}$$

Again application of Green's formula leads to

$$\begin{aligned} &\oint\limits_C \left[\xi_2(\xi_3 - m_3)n_2 - \xi_2(\xi_2 - m_2)n_3\right]\mathrm{d}C \\ &= \int\limits_A \left\{[\xi_2(\xi_3 - m_3)]_{,2} - [\xi_2(\xi_2 - m_2)]_{,3}\,\right\}\mathrm{d}A \\ &= \int\limits_A (\xi_3 - m_3)\;\mathrm{d}A \;=\; -(m_3 - s_3)\,A \end{aligned} \tag{A.13}$$

which proofs $(47)_1$ along with $(46)_1$ for $\alpha = 3$.

In an analogous way one obtains

$$\int\limits_A \tilde{w}_{,3}\;\mathrm{d}A = -\int\limits_A (\xi_2 - m_2)\;\mathrm{d}A = (m_2 - s_2)\,A \tag{A.14}$$

which yields the case $\alpha = 2$ in $(47)_1$.

Finally the integral $(47)_2$ is reformulated

$$\begin{aligned}
&\int_A (\tilde{\xi}_2^2 + \tilde{\xi}_3^2)\, \mathrm{d}A \\
&= \int_A (\xi_2^2 + \xi_3^2 + 2\xi_2\tilde{w}_{,3} - 2\xi_3\tilde{w}_{,2} + \tilde{w}^2{}_{,2} + \tilde{w}^2{}_{,3})\, \mathrm{d}A \\
&= \int_A [(\xi_2 - m_2)^2 + (\xi_3 - m_3)^2 + \xi_2 m_2 + \xi_3 m_3 + \xi_2\tilde{w}_{,3} - \xi_3\tilde{w}_{,2}]\, \mathrm{d}A \\
&+ \int_A [m_2(\xi_2 - m_2) + m_3(\xi_3 - m_3)]\, \mathrm{d}A \\
&+ \int_A [\tilde{w}_{,2}\,(-\xi_3 + \tilde{w}_{,2}) + \tilde{w}_{,3}\,(\xi_2 + \tilde{w}_{,3})]\, \mathrm{d}A\,.
\end{aligned} \tag{A.15}$$

The second integral in (A.15) using (A.11) – (A.14) yields

$$\int_A [m_2(\xi_2 - m_2) + m_3(\xi_3 - m_3)]\, \mathrm{d}A = \int_A [-\tilde{w}_{,3}\, m_2 + \tilde{w}_{,2}\, m_3]\, \mathrm{d}A \tag{A.16}$$

and the third integral is reformulated with $(4)_1$ and Green's formula

$$\begin{aligned}
&\int_A [\tilde{w}_{,2}\,(-\xi_3 + \tilde{w}_{,2}) + \tilde{w}_{,3}\,(\xi_2 + \tilde{w}_{,3})]\, \mathrm{d}A \\
&= \int_A \{[\tilde{w}(-\xi_3 + \tilde{w}_{,2})]_{,2} + [\tilde{w}(\xi_2 + \tilde{w}_{,3})]_{,3}\}\, \mathrm{d}A \\
&= \oint_C \tilde{w}[(-\xi_3 + \tilde{w}_{,2})n_2 + (\xi_2 + \tilde{w}_{,3})n_3]\, \mathrm{d}C\,.
\end{aligned} \tag{A.17}$$

Hence considering boundary condition $(4)_2$ and again application of Green's formula leads to

$$\begin{aligned}
&\oint_C \tilde{w}[(-\xi_3 + \tilde{w}_{,2})n_2 + (\xi_2 + \tilde{w}_{,3})n_3]\, \mathrm{d}C = \oint_C \tilde{w}\,(-m_3 n_2 + m_2 n_3)\, \mathrm{d}C \\
&= \int_A [-m_3\tilde{w}_{,2} + m_2\tilde{w}_{,3}]\, \mathrm{d}A
\end{aligned} \tag{A.18}$$

Furthermore using (A.11) – (A.14) one obtains

$$\int_A [-m_3\tilde{w}_{,2} + m_2\tilde{w}_{,3}]\, \mathrm{d}A = \int_A [-m_3(\xi_3 - m_3) - m_2(\xi_2 - m_2)]\, \mathrm{d}A \tag{A.19}$$

Thus the final version of (A.15) is obtained using (A.16), (A.19) and the

definition of the Saint–Venant torsion modulus $(46)_3$

$$\int_A (\tilde{\xi}_2^2 + \tilde{\xi}_3^2)\,\mathrm{d}A = \int_A [(\xi_2 - m_2)^2 + (\xi_3 - m_3)^2 + \tilde{w}_{,3}\,(\xi_2 - m_2) - \tilde{w}_{,2}\,(\xi_3 - m_3)]\,\mathrm{d}A$$
$$+ \int_A (m_2^2 + m_3^2)\,\mathrm{d}A \;=\; I_T + A(m_2^2 + m_3^2)\,. \tag{A.20}$$

## References


[1] J.H. Argyris, P.C. Dunne and D.W. Scharpf, On large displacement–small strain analysis of structures with rotational degrees of freedom, Comp. Meth. Appl. Mech. Engrg. 14 (1978) 401–451. 1, 3.2, 3.2

[2] J.H. Argyris, P.C. Dunne, G.A. Malejannakis and D.W. Scharpf, On large displacement–small strain analysis of structures with rotational degrees of freedom, Comp. Meth. Appl. Mech. Engrg. 15 (1978) 99–135. 1, 3.2, 6.1

[3] J.H. Argyris, O. Hilpert, G.A. Malejannakis and D.W. Scharpf, On the geometrical stiffness of a beam in space– A consistent v.w. approach, Comp. Meth. Appl. Mech. Engrg. 20 (1979) 105–131. 1, 3.2

[4] K.J. Bathe and S. Bolourchi, Large displacement analysis of three–dimensional beam structures, Int. J. Num. Meth. Engng. 14 (1979) 961–986. 1

[5] T. Belytschko and B.J. Hsieh, Non–linear finite element analysis with convected coordinates, Int. J. Num. Meth. Engng. 7 (1973) 255–271. 1

[6] M.A. Crisfield, A consistent co–rotational Formulation for non–linear three–dimensional beam elements, Comp. Meth. Appl. Mech. Engrg. 81 (1990) 131–150. 1

[7] B. Nour–Omid and C.C. Rankin, Finite rotation analysis and consistent linearization using projectors, Comp. Meth. Appl. Mech. Engrg. 93 (1991) 353–384. 1, 6.1, 6.2

[8] E. Reissner, On finite deformations of space–curved beams, J. Appl. Math. Phys. (ZAMP) 32 (1981) 734–744. 1, 3.1, 1

[9] J.C. Simo and L. Vu–Quoc, Three–dimensional finite–strain rod model. Part II: Computational aspects, Comp. Meth. Appl. Mech. Engrg. 58(1) (1986) 79–116. 1, 1, 6.1, 6.1

[10] J.C. Simo and L. Vu–Quoc, A geometrically–exact rod model incorporating shear and torsion–warping deformation, Int. J. Solids Structures 27(3) (1991) 371–393. 1

[11] A. Cordona and M. Géradin, A beam finite element non–linear theory with finite rotations, Int. J. Num. Meth. Engng. 26 (1988) 2403–2438. 1, 1

[12] A. Ibrahimbegović, Computational aspects of vector–like parametrization of three–dimensional finite rotations, Int. J. Num. Meth. Engng. 38 (1995) 3653–3673. 1, 1

[13] E. Reissner, Some considerations on the problem of torsion and flexure of prismatical beams, Int. J. Solids Structures 15 (1979) 41–53. 1

[14] E. Reissner, Further considerations on the problem of torsion and flexure of prismatical beams, Int. J. Solids Structures 19(5) (1983) 385–392. 1

[15] K.M. Weimar, Ein nichtlineares Balkenelement mit Anwendung als Längssteifen axialbelasteter Kreiszylinder, Report No. 10, Institut für Baustatik der Universität Stuttgart (1989). 1

[16] F. Gruttmann, S. Klinkel and W. Wagner, A finite rotation shell theory with application to composite structures, Revue européenne des éléments finis 4 (1995) 597–631. 1, 6.3

[17] J. Argyris, An excursion into large rotations, Comp. Meth. Appl. Mech. Engrg. 32 (1982) 85–155. 2, 3.2, A.1

[18] M. Géradin and D. Rixen, Parametrization of finite rotations in computational dynamics: a review, Revue européenne des éléments finis, 4 (1995) 497–553 2

[19] I.S. Sokolnikoff, Mathematical Theory of Elasticity, (McGraw–Hill, New York 1956). 2

[20] S.S. Antman, The theory of rods, Handbuch der Physik, Volume VIa/2 (Springer, Berlin. 1972). 3.1

[21] J.C. Simo, The (symmetric) Hessian for geometrically nonlinear models in solid mechanics: Intrinsic definition and geometric interpretation, Comp. Meth. Appl. Mech. Engrg. 96 (1992) 189–200. 3.2

[22] C. Truesdell and W. Noll, The nonlinear field theories of mechanics, in S. Flügge, Ed., Handbuch der Physik Volume III/3 (Springer, Berlin 1965). 4

[23] O.C. Zienkiewicz and R.L. Taylor, The Finite Element Method, 4th edition, Volume 1 (McGraw Hill, London, 1988). 5, 6

[24] G.M. Stanley, K.C. Park and T.J.R. Hughes, Continuum–based resultant shell elements, in: Finite Element methods for plate and shell structures, Vol. 1: Element technology, ed. T.J.R. Hughes, E. Hinton, Pineridge Press, Swansea, UK (1986). A.1